Acta Mech
https://doi.org/10.1007/s00707-024-04146-z

ORIGINAL PAPER

Marta Gruca · Marek Bukowicki · Maria L. Ekiel-Jeżewska

Brinkman-medium resistance hampers periodic motions of sedimenting particles

Received: 21 April 2024 / Revised: 9 September 2024 / Accepted: 24 October 2024

Abstract The dynamics of groups of non-touching particles settling under gravity in a crowded fluid medium are studied at the zero Reynolds number. It is assumed that the fluid velocity satisfies the Brinkman–Debye–Büche equations, and the particle dynamics are described in terms of the point-force model. The systems of particles at vertices of two or four horizontal regular polygons are considered that in the Stokes flow for a very long time do not destabilize, i.e., all the particles stay close to each other, performing periodic or quasiperiodic motions. It is known that such motions, as invariant manifolds, are essential for groups of particles at random initial positions to survive for a very long time and not destabilize. This work demonstrates that when the medium permeability is decreased, periodic motions cease to exist, and groups of particles split into smaller subgroups, moving away from each other. This mechanism seems to facilitate particle transport in a permeable medium.

1 Introduction

Motion of micro-objects in a crowded fluid environment, including particle-swarm transport in fractures [1] [2] has been recently investigated for various systems. Understanding and predicting colloid transport and retention in water-saturated porous media is important for the protection of human and ecological health [3]. Swimming of microorganisms in complex fluids has been widely investigated [4]. Brinkman-Debye-Büche equations [5,6] are often used to describe a wide range of different fluid media with a crowded or complex environment, giving the first approximation of the dynamics of active particles, swimming microorganisms, or other micro-objects when a finite permeability does play a role [7–12].

This work investigates how the medium's permeability influences periodic and quasi-periodic motions at zero Reynolds number flow. The existence of periodic solutions for certain initial configurations is important because it is connected with the existence of long-lasting groups of particles, initially at a wide range of different but relatively close initial positions, and later performing quasi-periodic or chaotic motions that prevent the group destabilization. This relation is well-known for the particles sedimenting in the Stokes flow [13–16].

For the Stokes fluid, periodic orbits have been found for many different groups of several particles settling under gravity in unbounded fluid [17–27], and in periodic boundary conditions [28,29], including relatively close [30] or even very close configurations where lubrication effects are significant [31], also for pairs of disks [32] or for rods, disks and hemispheres [33]. Periodic motions have been also found for systems of many point-particles in configurations of 2 or 3 horizontal regular polygons [14–16]. For such systems, long-lasting quasi-periodic oscillations of all the particles were also found, in addition to chaotic scattering, previously reported for three point-particles [13,34].

Marta Gruca and Marek Bukowicki contributed equally to this work.

M. Gruca · M. L. Ekiel-Jeżewska (✉) · M. Bukowicki
Institute of Fundamental Technological Research, Polish Academy of Sciences, Pawinskiego 5 B, 02-106 Warsaw, Poland
E-mail: mekiel@ippt.pan.pl

Published online: 16 December 2024

Therefore, in this work, we study periodic and quasiperiodic motions of groups of identical non-touching particles in regular configurations settling under gravity in the Brinkman medium, with the fluid flow described by the Brinkman-Debye-Büche equations, and the particle dynamics approximated by the point-force model. The plan of the paper is the following. In Sect. 2 we present the theoretical description. In Sect. 3 we introduce two families of the initial configurations, with 2 and 4 horizontal regular polygons (in the following called 'rings'). We also provide the equations of motion for their regular dynamics. The stationary configuration of a single horizontal ring is analyzed in Sect. 4. Periodic motion of two horizontal rings is discussed in Sect. 5, and long-time behavior of four horizontal rings in Sect. 6. Conclusions are presented in Sect. 7.

2 Theoretical description of the fluid and particle motion

2.1 Brinkman-Debye-Büche equations for the fluid flow

The dynamics of fluid in permeable media is described with the Brinkman-Debye-Büche (BDB) equations [5,6] for the fluid velocity $\boldsymbol{v}(\boldsymbol{r})$ and pressure $p(\boldsymbol{r})$ inside the permeable medium. In the presence of the system of N identical point particles, the BDB equations are given by:

$$\eta\left[\nabla^2\boldsymbol{v}(\boldsymbol{r})-\kappa^2\boldsymbol{v}(\boldsymbol{r})\right]-\nabla p(\boldsymbol{r})=-\sum_{i=1}^{N}\frac{\boldsymbol{G}}{N}\,\delta(\boldsymbol{r}-\boldsymbol{r}_i), \tag{1}$$

$$\nabla\cdot\boldsymbol{v}(\boldsymbol{r})=0. \tag{2}$$

where $1/\kappa^2$ is the permeability coefficient ($1/\kappa$ is the characteristic screening length), η is the fluid dynamic viscosity, $\boldsymbol{r}_i$ is the position of i-th particle and $\boldsymbol{G}/N$ is the external force exerted on a single particle ($\boldsymbol{G}=-G\hat{\boldsymbol{z}}$).

The fluid velocity $\boldsymbol{v}$ is expressed by the Green tensor $\boldsymbol{T}$,

$$\boldsymbol{v}(\boldsymbol{r})=\sum_{i=1}^{N}\boldsymbol{T}(\boldsymbol{r}-\boldsymbol{r}_i)\cdot\frac{\boldsymbol{G}}{N}, \tag{3}$$

$$\boldsymbol{T}(\boldsymbol{R})=\frac{1}{4\pi\eta R}\left(h_1(\kappa R)\boldsymbol{I}+h_2(\kappa R)\frac{\boldsymbol{R}\otimes\boldsymbol{R}}{R^2}\right), \tag{4}$$

where

$$h_1(\kappa R)=-\frac{1}{(\kappa R)^2}+\left(1+\frac{1}{\kappa R}+\frac{1}{(\kappa R)^2}\right)e^{-\kappa R}, \tag{5}$$

$$h_2(\kappa R)=\frac{3}{(\kappa R)^2}-\left(1+\frac{3}{\kappa R}+\frac{3}{(\kappa R)^2}\right)e^{-\kappa R} \tag{6}$$

and $R=|\boldsymbol{R}|$. The above fluid model will be called the Brinkman medium. Accordingly, the fluid flow generated by a single point-force $\boldsymbol{F}$ at $\boldsymbol{r}_i$, i.e., $\boldsymbol{T}(\boldsymbol{r}-\boldsymbol{r}_i)\cdot\boldsymbol{F}$, will be called a Brinkmanlet, in analogy to the Stokeslet [35].

2.2 Equations of motion for the particles

We consider N identical, spherical particles immersed in the Brinkman medium. We assume that their radius a_p is much smaller than the hydrodynamic screening length $1/\kappa$ (i.e., $\kappa a_p << 1$) [8,9]. The particles are well-separated from each other and we approximate them as point particles. The only forces acting on each particle are gravity $\boldsymbol{G}/N$ and the identical but opposite hydrodynamic resistance of the fluid. The velocity of i-th point particle has the form:

$$\frac{d\boldsymbol{r}_i}{dt}=\boldsymbol{u}_0+\sum_{j\neq i}\boldsymbol{T}(\boldsymbol{r}_{ij})\cdot\frac{\boldsymbol{G}}{N} \tag{7}$$

where $\boldsymbol{r}_{ij}=\boldsymbol{r}_i-\boldsymbol{r}_j$ and the Green tensor $\boldsymbol{T}(\boldsymbol{r}_{ij})$ is given by Eq. (4). Here $\boldsymbol{u}_0$ denotes the settling velocity of an isolated particle [5],

$$\boldsymbol{u}_0=[6\pi\eta a_p(1+\kappa a_p+(\kappa a_p)^2/3)]^{-1}\frac{\boldsymbol{G}}{N} \tag{8}$$

where a_p is the particle radius.

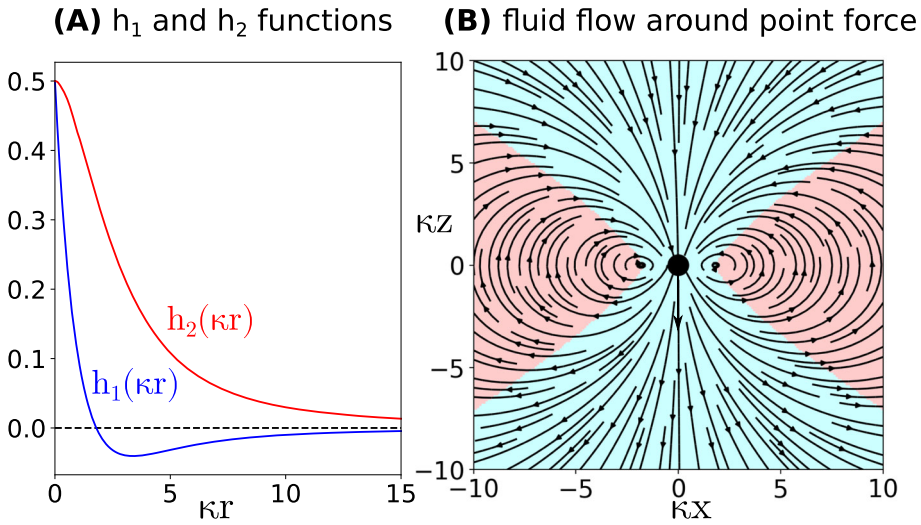

Fig. 1 Fluid flow around a point force settling in the Brinkman medium. **A** The dependence of h_1 and h_2 on κr given by Eqs. (5)–(6). **B** Fluid streamlines. The red color indicates regions where fluid moves upward

2.3 Basic properties

The fluid and particle dynamics depend on κ only through the rescaled variables: positions multiplied by κ, time multiplied by κ^2 and velocity divided by κ. In the limit $\kappa R \to 0$, the Green tensor $\boldsymbol{T}(\boldsymbol{R})$ given by Eq. (4) reduces to the Oseen tensor [35], as $\lim_{\kappa R\to 0} h_1(\kappa R) = \lim_{\kappa R\to 0} h_2(\kappa R) = 1/2$, and the Stokes dynamics is recovered.

However, for $\kappa R \gtrsim 1$ there appear some qualitative differences between the fluid and particle dynamics in a permeable medium and in a very viscous fluid [16]. It is important to notice that, unlike for the Stokes flow, the value of $h_1(\kappa r)$ may be negative, as shown in Fig. 1A. One of the effects is that, in the plane containing a particle and perpendicular to the force acting on it, at some points, the direction of the flow is opposite to the force. The regions where the flow generated by a single point force (with velocity given by Eq. (3) for $N = 1$) moves upward are colored red in Fig. 1B. The fluid streamlines for the Brinkmanlet are plotted there in a vertical plane xz containing the point force at the origin, with $\boldsymbol{r} = (x, 0, z)$ denoting the position of a fluid element. By comparing with the Stokeslet, we observe the qualitative difference: the Brinkmanlet streamlines are closed.

Applying the point-particle model (7) to the motion of two particles, we observe that in the Brinkman medium, two particles can settle slower than a single one, in a relatively wide range of relative positions marked in red in Fig. 1B. For other configurations, marked there in blue, pairs sediment faster than singlets, as in the Stokes flow. Moreover, a horizontal pair of closer particles can settle slower than a more separate horizontal pair, contrary to the behavior in the Stokes flow.

3 Model systems

3.1 Initial configurations of particles

We consider systems of many (N) particles arranged in $K = 1, 2,$ or 4 horizontal coaxial rings (regular polygons), each made of the same number of particles J. The initial conditions and the corresponding parameters for 2 and 4 rings are shown in Fig. 2. Initial configuration of both systems contains two identical regular polygons located exactly one above the other (with pairs of the particles aligned vertically). Therefore, the 2 rings system is a simple 3D generalization of the rectangle quartet, parameterized by C. In the case of a more complicated system of 4 rings, the additional two regular polygons, with different half-diameters (radii) R_2 and R_4, are located in the horizontal symmetry plane of the system. The vertices of both polygons have the same angular positions, in between the corresponding angular positions of the particles from the other two rings.

From now on, we will use dimensionless variables, based on an initial size of the group d as the length unit, and $G/(4\pi\eta d)$ as the velocity unit. Therefore, $4\pi\eta d^2/G$ is the time unit. From now on we will use the

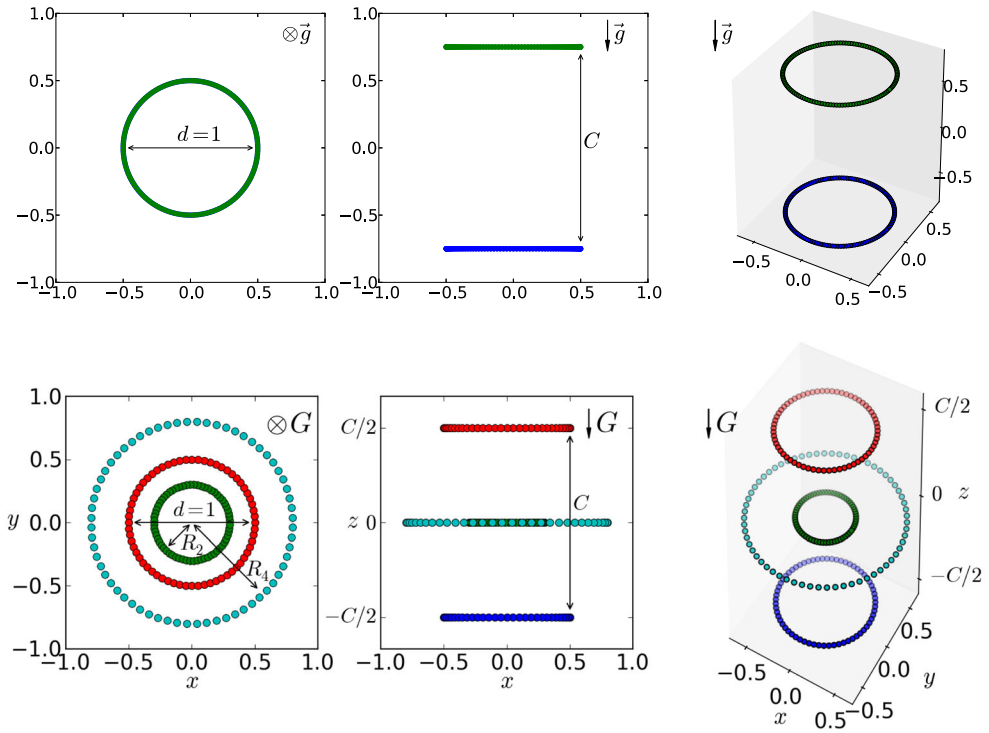

Fig. 2 Initial configurations of two systems made of $N=256$ particles (top, side, and 3D views). Top: two rings parameterized by C. Bottom: four rings parameterized by C, R_2 and R_4 as indicated. Reprinted with permission from [15]

following dimensionless quantities,

$$\tilde{\kappa} = \kappa d, \qquad \tilde{\boldsymbol{r}}_i = \frac{\boldsymbol{r}_i}{d}, \qquad \tilde{\boldsymbol{v}} = \frac{4\pi\eta d}{G}\boldsymbol{v}, \qquad \tilde{t} = \frac{G}{4\pi\eta d^2}t. \tag{9}$$

Here, d is the ring diameter, indicated in Fig. 2. Later on, we will use only the dimensionless quantities and therefore the tilde sign will be omitted.

For the symmetric systems of K coaxial rings made of J particles each, and $N = KJ$, it is convenient to describe the position of each particle $i = 1, ..., N$ using the cylindrical coordinates,

$$\boldsymbol{r}_i = (\rho_i \cos\phi_i, \rho_i \sin\phi_i, z_i), \tag{10}$$

with the sense of the z axis opposite to gravity,

$$\boldsymbol{G} = (0, 0, -G). \tag{11}$$

Denoting the label of the ring with $k = 1, ..., K$ and the label of the particle in the ring with $j = 1, ..., J$, we write $i = K(j-1)+k$.

Using this notation, we specify explicitly the initial configurations. For 2 rings,

$$\rho^{(0)}_{2(j-1)+k} = \frac{1}{2} \tag{12}$$

$$\phi^{(0)}_{2(j-1)+k} = \frac{2\pi(j-1)}{J} \tag{13}$$

$$z^{(0)}_{2(j-1)+k} = \begin{cases} \frac{C}{2}, & \text{if } k = 1 \\ -\frac{C}{2}, & \text{if } k = 2. \end{cases} \tag{14}$$

For 4 rings, the initial conditions are

$$\rho^{(0)}_{4(j-1)+k} = \begin{cases} \frac{1}{2}, & \text{if } k = 1, 3, \\ R_2, & \text{if } k = 2, \\ R_4, & \text{if } k = 4, \end{cases} \tag{15}$$

$$\phi^{(0)}_{4(j-1)+k} = \begin{cases} \frac{2\pi(j-1)}{J}, & \text{if } k = 1, 3, \\ \frac{2\pi(j-1)+\pi}{J}, & \text{if } k = 2, 4, \end{cases} \tag{16}$$

$$z^{(0)}_{4(j-1)+k} = \begin{cases} \frac{C}{2}, & \text{if } k = 1, \\ 0, & \text{if } k = 2, 4, \\ -\frac{C}{2}, & \text{if } k = 3. \end{cases} \tag{17}$$

3.2 Symmetric dynamics

To study stationary and periodic solutions of K rings, we will analyze the symmetric dynamics, assuming that

$$\phi_i(t) = \phi_i(0), \tag{18}$$

and that both radial and vertical coordinates of the particles from the same ring k are the same,

$$\rho_{K(j-1)+k}(t) = \rho_k(t), \tag{19}$$

$$z_{K(j-1)+k}(t) = z_k(t), \tag{20}$$

with $k = 1, ..., K$, $j = 1, ..., J$ and the total number of particles $N = KJ$. In this way, each ring k is represented by the particle with the label $i = k$. For the symmetric dynamics, the equations of the motion (7) reduce to the following system of $2K$ equations for ρ_l and z_l, with $l = 1, ..., K$,

$$\frac{d\rho_l}{dt} = -\frac{1}{KJ}\sum_{k=1}^{K}\sum_{j=1}^{J}(1-\delta_{kl}\delta_{j1})\frac{(z_k-z_l)\left[\rho_k\cos\left(\phi_{K(j-1)+k}-\phi_l\right)-\rho_l\right]}{R^3_{lkj}}h_2(\kappa R_{lkj}), \tag{21}$$

$$\frac{dz_l}{dt} = -u_0 - \frac{1}{KJ}\sum_{k=1}^{K}\sum_{j=1}^{J}(1-\delta_{kl}\delta_{j1})\left(h_1(\kappa R_{lkj})\frac{1}{R_{lkj}} + h_2(\kappa R_{lkj})\frac{(z_k-z_l)^2}{R^3_{lkj}}\right), \tag{22}$$

$$R^2_{lkj} = (z_k - z_l)^2 + \rho_l^2 + \rho_k^2 - 2\rho_l\rho_k\cos\left(\phi_{K(j-1)+k} - \phi_l\right), \tag{23}$$

where $u_0 = |\boldsymbol{u}_0|$ is determined by Eq. (8), normalized with the use of Eq. (9), and with the choice $a_p = d\sin\frac{\pi}{N}/2$,

$$u_0 = \frac{4}{3N\sin(\pi/N)}\left[\left(1 + \kappa d\sin\frac{\pi}{N}/2 + \left(\kappa d\sin\frac{\pi}{N}/2\right)^2/3\right)\right]^{-1} \tag{24}$$

The dynamics are solved numerically in the reference frame moving with $\boldsymbol{u}_0$.

4 Stationary configurations of a single ring and their settling speeds

From the dynamics (18)–(23) it follows that a single ring (particles at vertices of a horizontal regular polygon) is the stationary configuration, as in the case of the Stokes flow [18]. The settling velocity V_z of a single ring made of N particles can be easily found from Eq. (22),

$$V_z = -u_0 - \frac{1}{N}\sum_{j=2}^{N}\frac{h_1(\kappa R_{1j})}{R_{1j}} \tag{25}$$

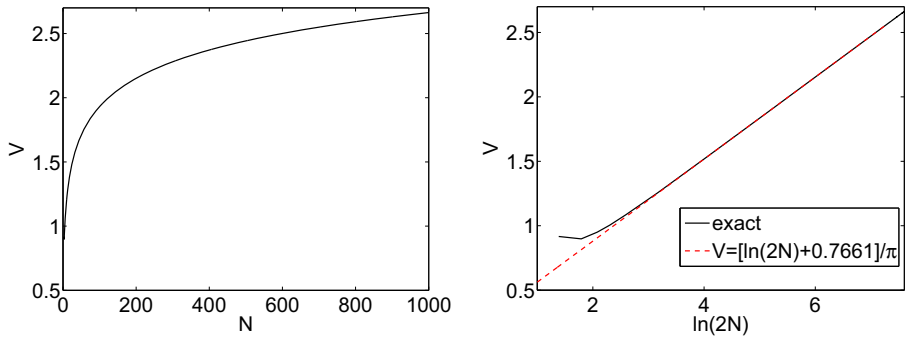

Fig. 3 Velocity (the absolute value V) of a ring with diameter d, settling under the gravitational force $\boldsymbol{G}$ in the Stokes fluid. The ring is made of different numbers N of point particles. Velocity is normalized by $G/(4\pi\eta d)$. Increasing N decreases the distance between consecutive point particles within the ring while d and $\boldsymbol{G}$ are fixed

where u_0 is given by Eq. (24) and

$$R_{1j} = \sqrt{\frac{1-\cos\left(\frac{2\pi(j-1)}{N}\right)}{2}}. \tag{26}$$

In the Brinkman medium, the horizontal ring keeps the same size and orientation while settling, by the same reversibility arguments as in the Stokes flow.

4.1 Stationary configurations a single ring in the Stokesian dynamics

It is useful to analyze the settling velocity V_z of a single horizontal ring made of N touching spherical beads, moving under gravity in the Stokes fluid. With the normalization introduced in Eq. (9) (in particular, the ring diameter taken as the length unit),

$$V_z = -\frac{4}{3N\sin\frac{\pi}{N}} - \frac{1}{N}\sum_{j=2}^{N}\frac{1}{2R_{1j}}. \tag{27}$$

The dependence of the absolute value $V = |V_z|$ of the settling velocity V_z on the number of particles N in the ring is plotted in Fig. 3. It is clear that for larger numbers of particles, even as small as $N \geq 8$, the settling velocity V scales logarithmically with N,

$$V \approx \frac{1}{\pi}\left[\ln(2N) + 0.7661\right] \qquad \text{for } N \to \infty. \tag{28}$$

In the literature, such logarithmic relations for the mobility coefficients of a thin ring in the Stokes flow were derived analytically [36–39]. For the axisymmetric motion of a ring of length l and cross-sectional radius $b \ll l$,

$$V = \frac{1}{\pi}\left(\ln\frac{l}{b} + K\right), \tag{29}$$

with the normalization from Eq. (9). The slope does not depend on the specific geometry of the ring. However, the constant K does; for example, in the case of a bent spheroid, it is different than in the case of a torus or bent cylinder [36–39]. In Eq. (28), we provide the value of K for the ring made of spherical beads, in the point-force approximation.

Table 1 The value of $\kappa\rho_0$ for which the absolute value V of the settling velocity of a single ring of N particles reaches the minimum (for fixed a_p, κ and N)

N	8	16	32	64	128	256	1000
$\kappa\rho_0$	1.83	2.81	5.21	10.6	21.4	43.0	168.2

4.2 Stationary configurations a single ring in the Brinkman medium

As discussed in Sect. 2.3, the function $h_1(x)/x$ becomes negative for sufficiently large values of x, and reaches a minimum there. Therefore, a horizontal ring of particles may settle down slower than the single particle, which depends on the number of particles N, the ring radius ρ_0, and the hydrodynamic screening coefficient κ. Another consequence is that a smaller ring may settle down slower than a bigger one made of the same particles.

For given a_p, N and κ, there exists such $\rho = \rho_0$ for which the absolute value of the settling velocity of the ring is the smallest. For ρ smaller than ρ_0 the relation from Stokes fluid is kept: smaller rings settle faster than bigger ones.[1] In the opposite - 'atypical' - situation, when ρ is greater than ρ_0, this relation is reversed: bigger rings settle down faster. In Table 1, the critical values of ρ_0 are presented, for which the absolute value of the settling velocity is the smallest. From the data in Table 1 it follows that $\kappa\rho_0$ increases with N approximately linearly. Moreover, if the considered sizes of the rings are fixed, for larger numbers of particles, atypical behavior is shifted to larger values of κ, approximately proportional to N. Note that although the second term in Eq. (25) can be positive, but V_z is negative - the total velocity always has the same direction as gravity.

5 Two rings in the Brinkman medium

In this section, we analyze how the resistance of the Brinkman medium affects the existence of periodic solutions for the system of two rings. For a given number of particles N and inverse hydrodynamic screening length κ, the initial configurations are specified by a single geometrical parameter C.

The case of a single ring of particles, discussed in Sect. 4.2, can be used as a useful reference point for understanding the dynamics of two or more rings, especially the breaking of the system for some values of the parameters. The important property is that a smaller ring may settle down slower than a bigger one made of the same particles. This effect allows for breakage of the system of several rings: due to the difference in settling velocities between the bottom bigger and upper smaller rings, the distance between them will increase. This type of decay is not possible in the Stokes fluid.

Properties of the function $h_1(x)/x$ and the dynamics of a single ring, described in Secs. 2.3 and 4.2, have significant consequences for the behavior of two rings. In the Stokes flow two rings made of the same number of identical particles initially exactly one above the other perform periodic motions if $C > C_0$, or slowly expand horizontally (with the upper ring smaller than the bottom one) if $C < C_0$ [14,15]. The critical value of C_0 depends on N.

In the Brinkman medium, two rings can perform periodic oscillations or horizontal expansion (as in the Stokes flow) or exhibit a new behavior: move away from each other vertically. Since for some values of N and κ a bigger ring settles down faster than a smaller one, the smaller ring may be left behind. This mechanism is important for the vertical separation of the rings, because at the first stage of the dynamics, the radius of the upper ring is decreasing, while the radius of the bottom one-increasing. The nature of the decay of the two-ring system described here is different from the ring expansion for $C < C_0$. In the last case, the vertical distance between two rings does not increase with time.

Table 2 presents the parameters that lead to periodic oscillations or decay (i.e., two rings moving away from each other vertically), for a chosen value of $C = 1.5$. The critical values of κ for which we observe the decay are greater for a bigger number of particles N. The critical values of κ might be proportional to the critical value of N, in agreement with the linear relation in Table 1. To check this statement, much more simulations would be needed. The transition between periodic oscillations and decay for increasing values of κ is illustrated in Fig. 4. For $\kappa \geq 10$, the slower smaller ring is left behind the faster larger ring.

[1] In the Stokes flow, for a fixed number N of the particles in the ring, and a fixed total force $\boldsymbol{G}$ exerted on the ring, equation (28), now normalized with the use of a fixed length scale rather than the ring diameter d, determines the ring velocity proportional to d^{-1}.

Table 2 The oscillation period T of two rings made of N particles, sedimenting in the Brinkman medium with the screening length κ, initially with $C = 1.5$. Decay of the cluster takes place for smaller N and larger κ

κ	$N=8$	$N=32$	$N=64$	$N=256$
0.5	43.6	28.8	25.2	20.8
1	57.2	34	29.6	24
2	154.4	52.8	43.6	34
5	Decay	208.4	123.6	81.2
10	Decay	Decay	383.6	184.8
20	Decay	Decay	Decay	454.8
50	Decay	Decay	Decay	2044

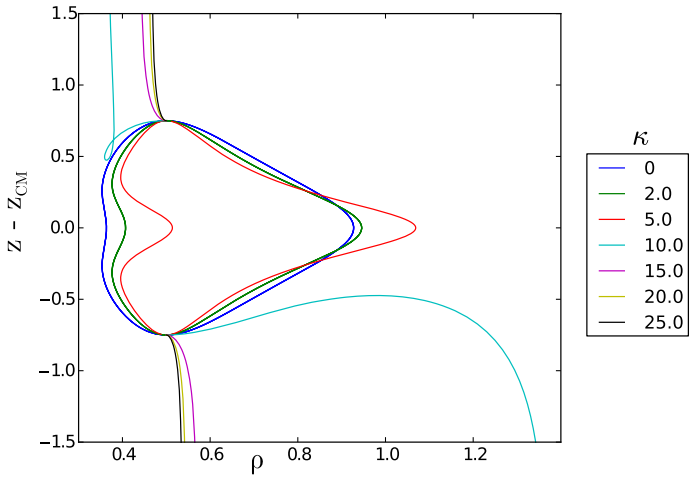

Fig. 4 Trajectories of particles 1 and 2 from two rings with $N = 32$ and $C = 1.5$, in the center-of-mass reference frame, for different κ. For $\kappa \geq 10$, the two rings move away from each other vertically

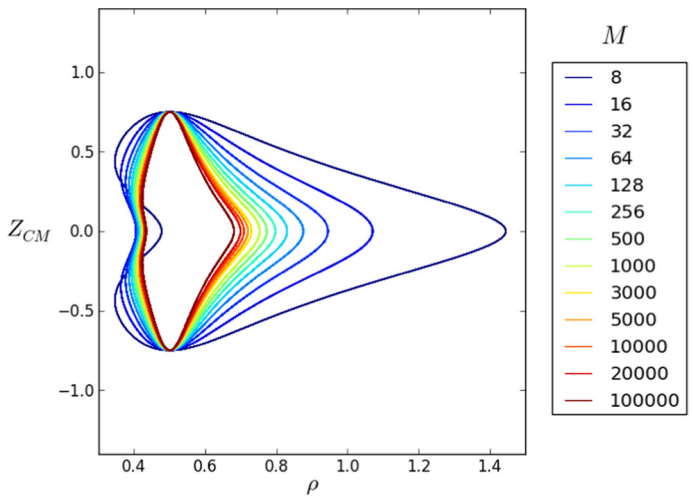

Fig. 5 Trajectories of particles from two rings in the center-of-mass frame for $C = 1.5$, $\kappa = 2$ and different particle numbers M

The dependence of shapes of periodic trajectories on N is shown in Fig. 5. For the increasing values of N, the change of the trajectory shape is qualitatively similar (but not the same) to the change of shape for the increasing value of κ. Similarly as in the Stokes fluid [15], trajectories of particles in the system with smaller N are more elongated in the horizontal direction, as shown in Fig. 5. Consistently with the elongation and a larger length of the trajectories, for a smaller number of particles, the period of the motion is larger (see Table 2). The dependence of the periodic trajectory on the initial configuration, i.e. on C, is illustrated in Fig. 6. It is similar to the one for the Stokes fluid [15], even though $\kappa = 2$ is not very small.

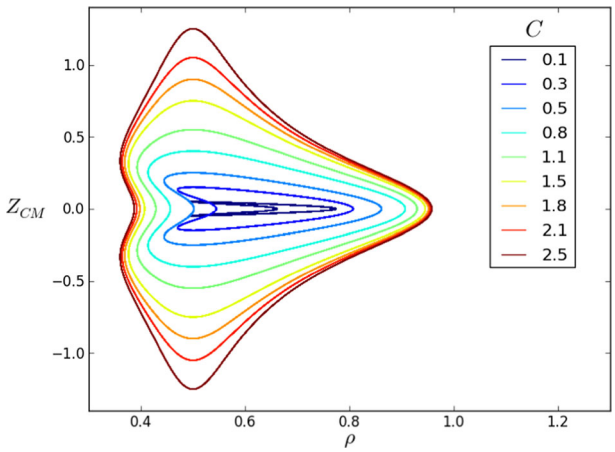

Fig. 6 Trajectories of particles from two rings in the center-of-mass frame for $N = 32$, $\kappa = 2$ and different values of C

Summarizing, the periodic motions of two rings in the Brinkman medium and Stokes fluid are similar. However, their existence is restricted only to sufficiently small values of κ. The range of κ with periodic motions of two rings systematically increases with the increase of the particle number. Smaller clusters destabilize for a more permeable medium.

6 Four rings in the Binkman medium

It was shown [15,16] that in the Stokes flow dynamics of four rings are chaotic in a wide range of C, R_2 and R_4. In most cases, four rings decay after a short or a long time. However, three families of periodic orbits have been found for specific values of R_2 and R_4, dependent on C. In the parameter space $R_2 \times R_4$, the periodic solutions are surrounded by islands of almost periodic, or periodic with complex trajectories, long-lasting motions of the rings that stay close to each other, so as for a very long time the cluster does not decay [15,16].

In this section, we focus on the dependence of the dynamics of four rings on the inverse screening length κ. First, we study the range and properties of the periodic motions, and next, we analyze how the destabilization of four rings depends on κ.

6.1 Periodic motions

To find periodic orbits, we use the procedure described in Appendix A, and applied also in Refs [15,16] for the Stokes flow. We consider $N = 256$ and $C = 1.5$ and increase values of κ from zero systematically by step 0.02. The prior analysis of the two-ring system in permeable medium (in Sect. 5), as well as of four-rings in the Stokes flow [15] have shown that the results obtained for $N = 256$ and $C = 1.5$ are representative for wider ranges of these parameters.

For smaller values of κ, we find three families of periodic oscillations, similarly as in the Stokes flow [15,16]. For selected values of κ, examples of particle periodic trajectories in the center-of-mass frame for each family are shown in Fig. 7. For the 1st family, particles from all the rings follow the same trajectory. For the 2nd family, particles from rings 1, 2, and 3 follow the same (larger) trajectory, and the particles from ring 4 move along another (smaller) trajectory. For the 3rd family, particles from rings 1, 3, and 4 follow the same (larger) trajectory, and the particles from ring 2 move along another (smaller) trajectory.

Shapes of the trajectories do not change much when κ is increased from zero. For all three types of periodic solutions the trajectory width, defined as $max_{i\in\{1,\ldots,4\},t\in T}\ \rho_i\ (t) - min_{i\in\{1,\ldots,4\},t\in T}\ \rho_i\ (t)$, is consistently a bit smaller for larger values of κ. The largest changes in trajectory shape are observed for 1st periodic solution, where the range of κ is the widest. With decreasing permeability of the medium, mild bends of trajectory became sharper. In the case of 2nd type of solution, the shape and the width of the trajectory do not change significantly for different values of κ. For 3rd solution, the trajectory width decreases with larger κ, while the length of the trajectory of ring number 2 (in the middle) increases.

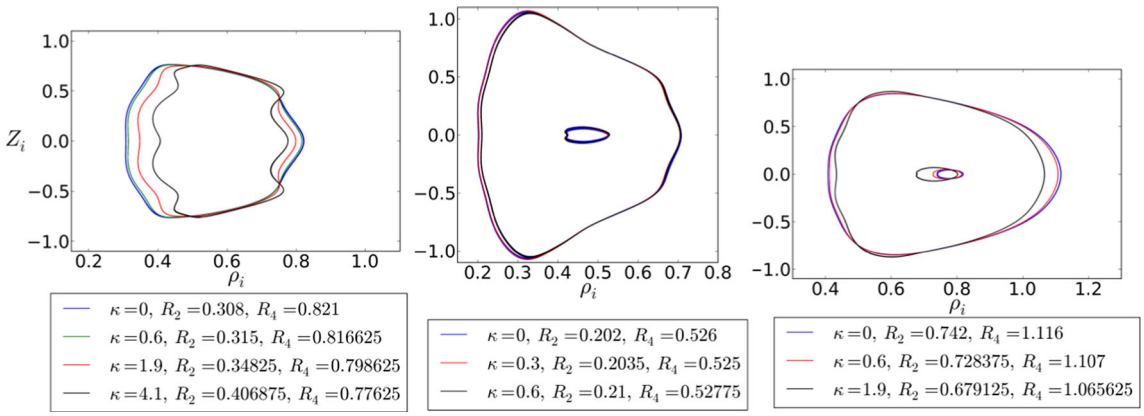

Fig. 7 Three families (1st, 2nd, and 3rd) of periodic trajectories of particles from four rings in the center-of-mass frame for the indicated values of κ and initial ring radii R_2 and R_4. Here $N = 256$ and $C = 1.5$

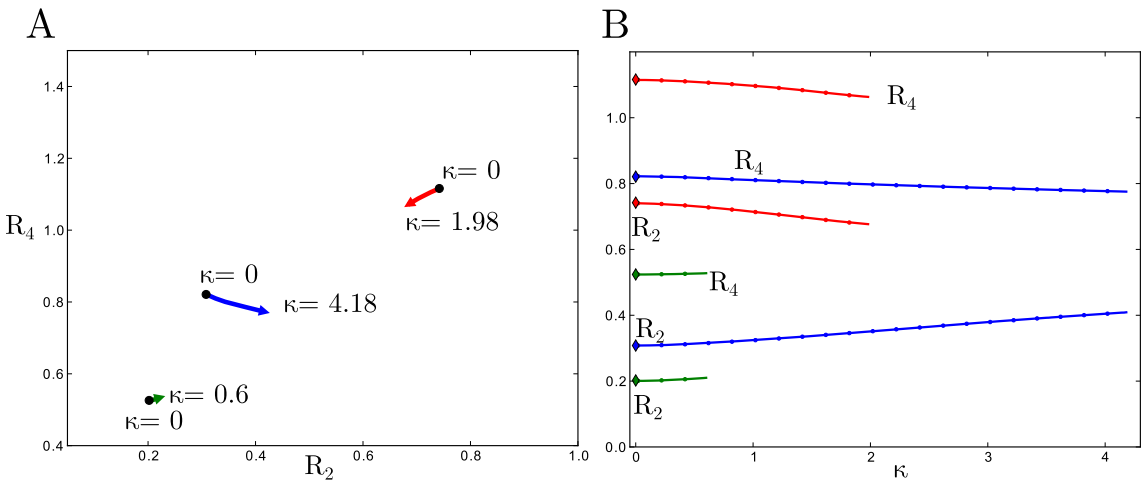

Fig. 8 The initial ring radii R_2 and R_4 for $N = 256$ and $C = 1.5$ corresponding to periodic solutions from the three families for different values of κ (changed by step 0.02): (A) shown in the phase space $R_2 \times R_4$, and (B) R_2 and R_4 plotted against κ. Colors correspond to different types of periodic solutions: blue: 1st, green: 2nd, and red: 3rd

The ring radii R_2 and R_4 corresponding to the periodic oscillations depend on κ, as indicated in the legends of Fig. 7. This relation is systematically investigated in Fig. 8. For larger values of κ, periodic motions from the three families shown in Fig. 7 cease to exist. The range of κ for which periodic trajectories were found is the widest in the case of 1st family of the periodic solution, up to $\kappa = 4.18$. This value is still significantly lower than for 2-ring system ($\kappa \approx 8$, Sect. 5). Periodic motions from the 2nd family can be found only for small values of $\kappa \leq 0.60$. Periodic solution of 3rd type exists for $\kappa \leq 1.98$. Approaching borders of these ranges of κ, almost periodic or periodic with complex trajectories motions exist for more and more narrow ranges of R_2 and R_4. In wider ranges of R_2 and R_4, the cluster made of four rings destabilizes. An analogous situation has been observed in the Stokes fluid for varying C and N [16]. The dependence of R_2 and R_4 on κ, shown in Fig. 8B, is reflected in trajectories shown in Fig. 7. It is visible that the trajectories of periodic solutions do not change significantly with changing permeability.

6.2 Cluster life times

As in the Stokes flow, in the Brinkman medium, the cluster made of four rings destabilizes for a wide range of R_2, R_4, and κ. Examples of the decay are shown in Fig. 9, for two clusters of two rings each (left), and for a single ring and a cluster made of three rings (right).

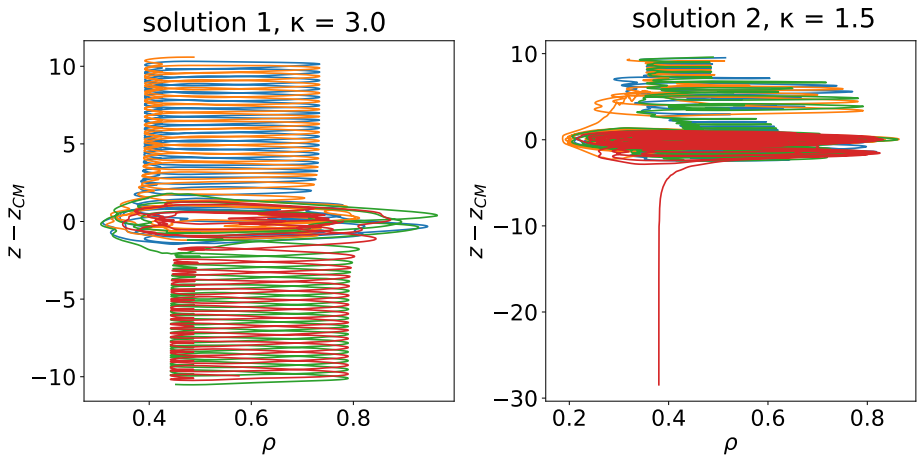

Fig. 9 Examples of decay of four rings with $N = 256$ and $C = 1.5$, settling under gravity in a permeable medium. Left: $R_2 = 0.24$, $R_4 = 0.58$. Right: $R_2 = 0.345$, $R_4 = 0.78$

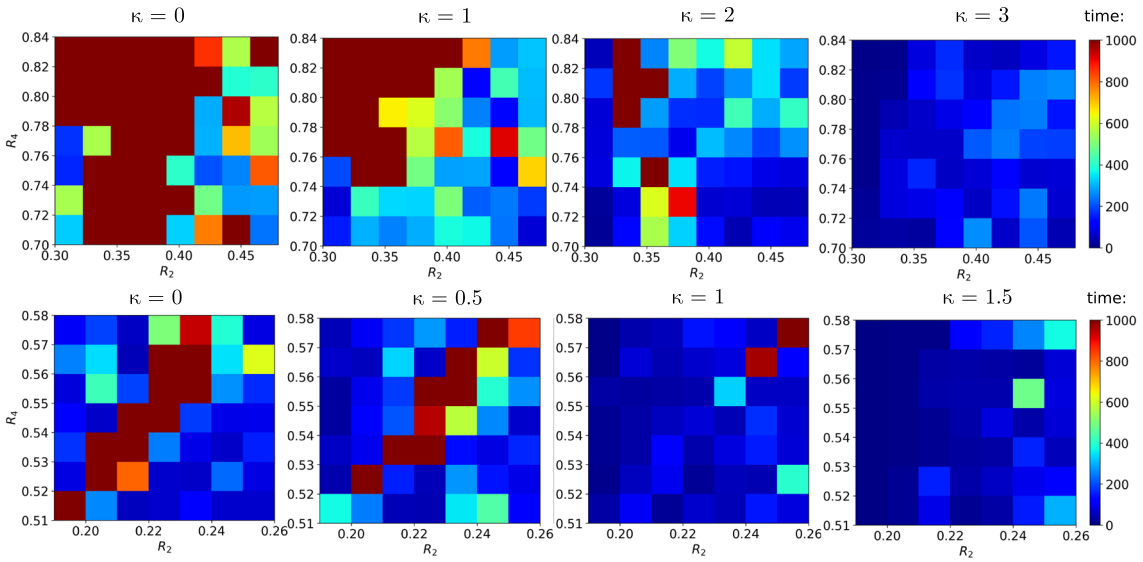

Fig. 10 Cluster lifetime (the time when the distance between top and bottom rings exceeds 2.5), shown in colors. The chosen ranges of R_2 and R_4 include the periodic solution 1 in the upper panel, and the periodic solution 2 in the lower panel. $N = 256$, $C = 1.5$

To quantify the destabilization process, we evaluate the cluster lifetime, estimated as the time when the distance between the top and bottom rings exceeds 2.5. Figure 10 shows the cluster lifetime for the increasing values of κ in two ranges of $\{R_2, R_4\}$. The first one includes the periodic solution 1, and the second one - the periodic solution 2 (if they exist).[2] For $\kappa = 0$, the periodic solutions are surrounded in the phase space of R_2 and R_4 by relatively large regions (brown) where the cluster does not destabilize until the end of the simulations. The rings perform almost periodic motions or periodic motions from a cascade of doubled periods. (an example of a period-doubling periodic trajectory for $\kappa = 0$ is shown in Appendix B.) Fig. 10 illustrates that the brown regions shrink when κ increases. Moreover, cluster lifetimes systematically decrease with the increasing κ.

Figures 11 and 12 illustrate that for larger values of κ, the long-lasting clusters are found in narrower ranges of R_2 and R_4. Moreover, for larger values of κ, the clusters that are out of this range destabilize faster (the cluster lifetime becomes shorter). The difference is even larger if the decay time is related to the number of oscillations or traveled distance because the motion of particles in a medium with larger κ is slower. As

[2] Periodic solutions are not always seen as brown spots in Fig. 10 because the grid is larger than the accuracy to determine them.

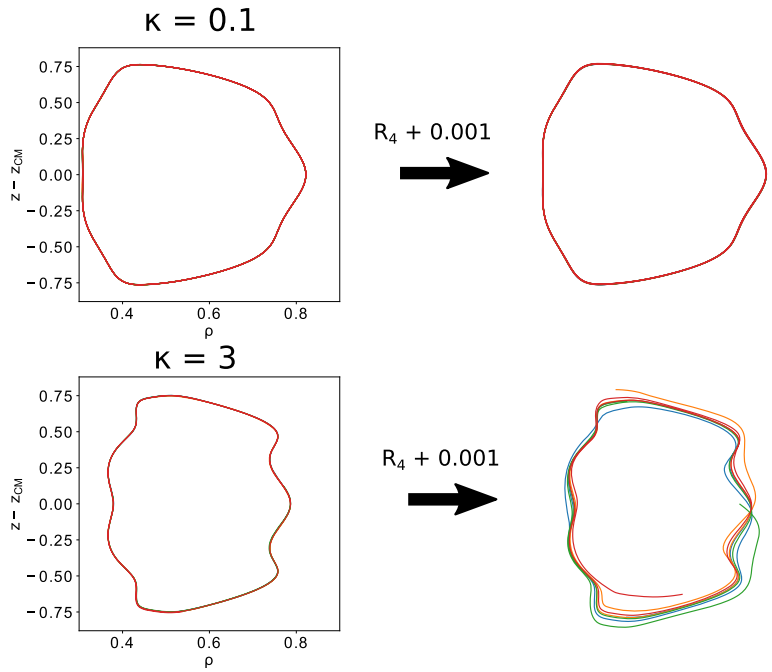

Fig. 11 Evolution of trajectories from the 1st family in the range of times [0, 100]. Again, $N = 256$, $C = 1.5$. Left column: the periodic trajectory for $\{R_2, R_4\} = \{0.308375, 0.822\}$ for $\kappa = 0.1$ and $\{R_2, R_4\} = \{0.379, 0.786625\}$ for $\kappa = 3$. Right column: the trajectories of all the particles for the same values of R_2 and κ but a bit larger value $R_4 + 0.001$

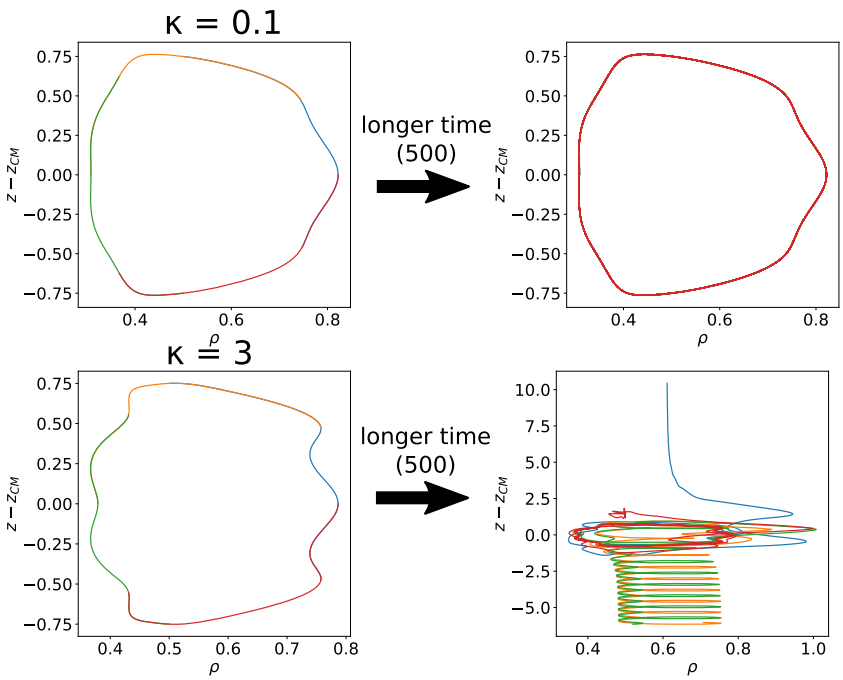

Fig. 12 As in Fig. 11, but for a wider range of times [0, 500]

Table 3 How do dynamics of clusters made of two or four rings depend on initial conditions?

	Stokes fluid	Brinkman medium
Do periodic orbits of two rings exist?	For aspect ratio $C > C_0$	For aspect ratio $C > C_0$ and small κ
Do periodic orbits of four rings exist?	For a few configurations	For a few configurations and small κ
Do all particles form a long-lasting cluster?	In large 'islands' close to periodic orbit	The 'islands' are smaller for larger κ
Is the dynamics chaotic?	For a wide range of initial conditions	The range shrinks with increasing κ

an example, two periodic solutions from the 1st family are considered for smaller and larger values of κ. An increase of R_4 by a very small number of 0.001 does not lead to decay of the cluster for $\kappa = 0.1$ (even though the orbit does not seem to be exactly periodic), but it leads to destabilization of the cluster for $\kappa = 3$.

7 Conclusions

In many systems found in nature or in technological contexts, micro-objects (particles, microorganisms, etc.) sediment in a more or less crowded environment-in a fluid with solid-like intrusions, which increase the effective friction force exerted on them by the fluid. Therefore, it is interesting to investigate how this increased friction affects basic features of many-body dynamics, known for Stokes fluids: chaotic scattering, related to the existence of periodic, usually unstable orbits, and the formation of long-lasting particle clusters. In this work, such a crowded environment has been modeled as the permeable medium. We have studied the sedimentation of many-particle systems in the Brinkman medium with decreasing values of permeability. The fluid motion has been described by the Brinkman-Debye-Bueche equations and the motion of particles by the corresponding point-force model. We have investigated the dynamics of many particles which initially form 2 or 4 coaxial horizontal rings. For large permeability, we have found a family of periodic orbits, analogical to those found in Stokes fluids; for smaller permeability, such solutions are absent and the systems of two or four rings do not form long-lasting clusters. The results of this work are summarized in Table 3. In Appendix C we present time-dependent velocities of periodic clusters made of two and four rings.

The existence of periodic solutions for the systems made of several coaxial horizontal regular polygons ('rings') may be important for the dynamics of sedimenting clouds of randomly distributed particles [14]. Destabilization of random clouds of particles has been widely investigated in the literature [40–42]. It has been shown that in the presence of a single solid plane wall, suspension drops destabilize faster and travel a smaller distance before the decay [43,44]. One would anticipate a similar effect for a fracture or pore with a more complex geometry of the walls surrounding the fluid [1]. Therefore, it could be expected that the resistance of the Brinkman medium tends to destabilize sedimenting groups of particles. Therefore, the results of this work might be useful for medical and industrial applications.

Funding M. L. E.-J. was supported in part by Narodowe Centrum Nauki (Grant number UMO-2021/41/B/ST8/04474).

Declarations

Conflict of interest The authors have no relevant financial or non-financial interests to disclose.

Appendix A: Procedure of finding periodic trajectories for κ>0

In the Stokes flow, to find periodic solutions for other values of C and N, the corresponding parameters R_2 and R_4 were searched for in the vicinity of the values corresponding to periodic solutions already known (for

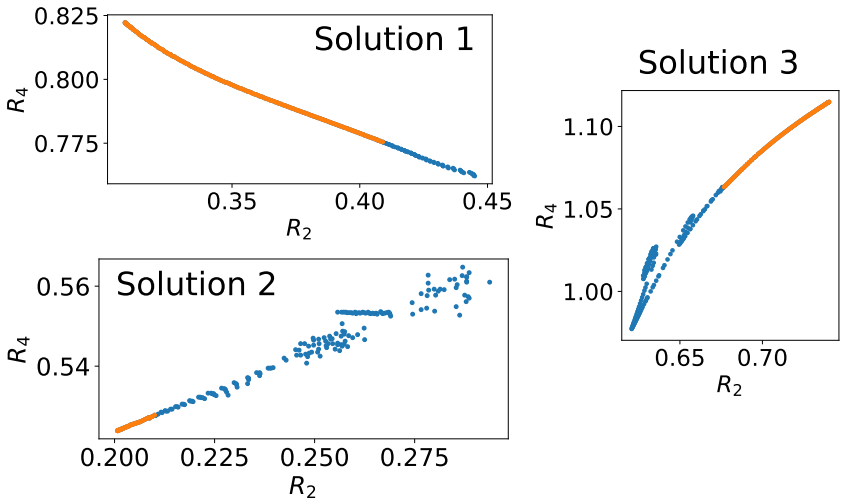

Fig. 13 Parameters R_2 and R_4 of the periodic solutions found for growing κ. It is visible that for large resistance of the Brinkman medium, the procedure fails to find a single periodic solution and meanders back and forth. Orange dots mark the conservative range where solutions are periodic for a long time (the same which is plotted in fig. 8)

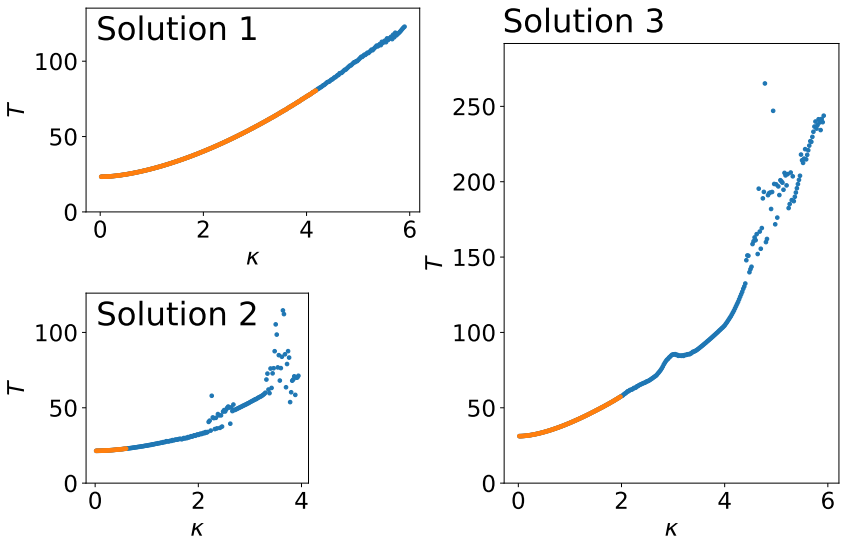

Fig. 14 Period of the motion for different κ and the three families of periodic solutions. Consistently for all data, larger resistance results in a longer period

$C = 1.5$, $N = 256$). After finding periodic solutions for new values of C or N the procedure was repeated iteratively with a new set of parameters as the new starting point. This method works well and allows, using small steps, to find solutions for parameters C and N even much different from the initial ones.

The detailed procedure of searching for periodic solutions was as follows [15,16]. Let us assume that there is a known periodic solution for C^A with parameters $R_2 = R_2^A$ and $R_4 = R_4^A$. Our aim is to find parameters $R_2 = R_2^B$, $R_4 = R_4^B$ of initial configuration corresponding to periodic solution of different C, $C = C^B$. If $|C^B - C^A|$ is small, we expect that R_2^B is close to R_2^A and R_4^B is close to R_4^A. In analysis performed in this study, $|C^B - C^A|$ was equal to 0.01. In the first step, 49 (7×7 grid) different initial configurations were examined. One of them, in the center of the

grid, was $\left(R_2^A, R_4^A\right)$. Initial configurations tested in the first step can be written as: $R_2 \in \left\{R_2^A + i\, d_{res}\right\}$, $R_4 \in \left\{R_4^A + j\, d_{res}\right\}$ where $i, j \in \{-3, ..., 3\}$ and d_{res} is a certain small number, resolution of the grid. In this study d_{res} was equal to 0.001. For all 49 initial configurations, a short simulation was performed, with a total time equal to $1.5T_A$, where T_A is the period for C^A. Positions of particles were recorded with very high resolution. Subsequently among these trajectories the one that is the closest to the periodic is chosen. More

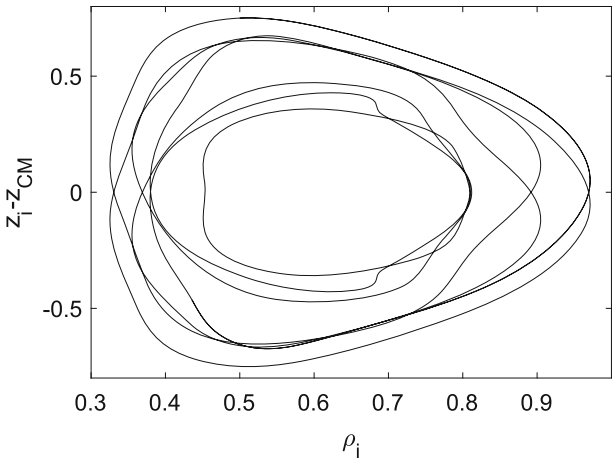

Fig. 15 Periodic trajectory followed by all the particles from 4 rings with $N = 64$, $C = 1.5$, $\kappa = 0.1$, $R_2 = 0.45325$ and $R_4 = 0.812$

precisely we measure the difference between the initial position of particles and the most similar configuration during the dynamics, excluding from this comparison time just after beginning, $t < \frac{T_A}{10}$. In this way, we find the best pair of $\left(R_2^B, R_4^B\right)$ parameters out of 49 examined. Having them identified, a new 7×7 grid of initial configurations is built, with the $\left(R_2^B, R_4^B, C^B\right)$ found in the previous step in the middle and resolution d_{res} equal to half of the value used before. In order to find the periodic solution for C^B, 5 such iterations are performed with final resolution $6.25 \cdot 10^{-5}$. $\left(R_2^B, R_4^B\right)$ parameters found in this way for C^B were used to start the whole procedure (for the next value of C, close one to C^B).
In the Brinkman medium, the same procedure was applied, but with C replaced by κ. The results are shown in Fig. 8 for a range of values where the existence of periodic orbits was confirmed. The results of this procedure are also shown in Fig. 13 (orange), together with the outcome for larger values of κ (blue). In Fig. 14 it is shown that the characteristic time T of the oscillations increases with the increase of κ.

Appendix B: An example of a complex periodic trajectory of four rings settling in the Brinkman medium

The procedure described in the previous Appendix does not allow to finding of more complex periodic trajectories, resulting from bifurcations that resemble the period-doubling cascade. An example of such periodic trajectory in the center-of-mass frame is shown in Fig. 15 for $N = 64$, $C = 1.5$. In the phase space of R_2 and R_4, this periodic solution is located close to the periodic solution from the 1st family. On a map similar to the ones shown in Fig. 10, it would belong to the interior of a brown 'island' of long-lasting clusters.
The trajectory shown in Fig. 15 closes after making 7 loops. The period of this motion is equal to $T = 145.14$, and therefore it is close to 7 times the period of the periodic solution from the 1st family, shown in Fig. 14. We have found many many closed periodic trajectories of this type, for different values of κ, including $\kappa = 0$. Even more common are trajectories of similar shapes with more loops, that are open at the end of the simulation time. It is not known if they close after a sufficiently long time or not. Anyhow, they all correspond to the clusters of four rings that do not destabilize during our simulations. The existence of such trajectories is related to the transition to chaos. The chaotic dynamics of four rings sedimenting in the Stokes flow were discussed in Refs. [15,16].

Appendix C: The settling velocity of 2 and 4 coaxial rings in the Brinkman medium

In Fig. 16, the time-dependent settling velocities of systems made of two rings during one period are shown, for the center of mass of the system and for each ring separately, for different values of C, N, and κ. The settling velocities depend on u_0. Here we use u_0 defined in Eq. (24). The results are shown for the settling velocity that includes u_0 and without the contribution of the self-term. For larger κ the difference between the instantaneous settling velocities of the two rings is smaller. This tendency is kept for κ much larger than presented in the Fig. 16, providing that the motion is periodic (what requires a larger number of particles).

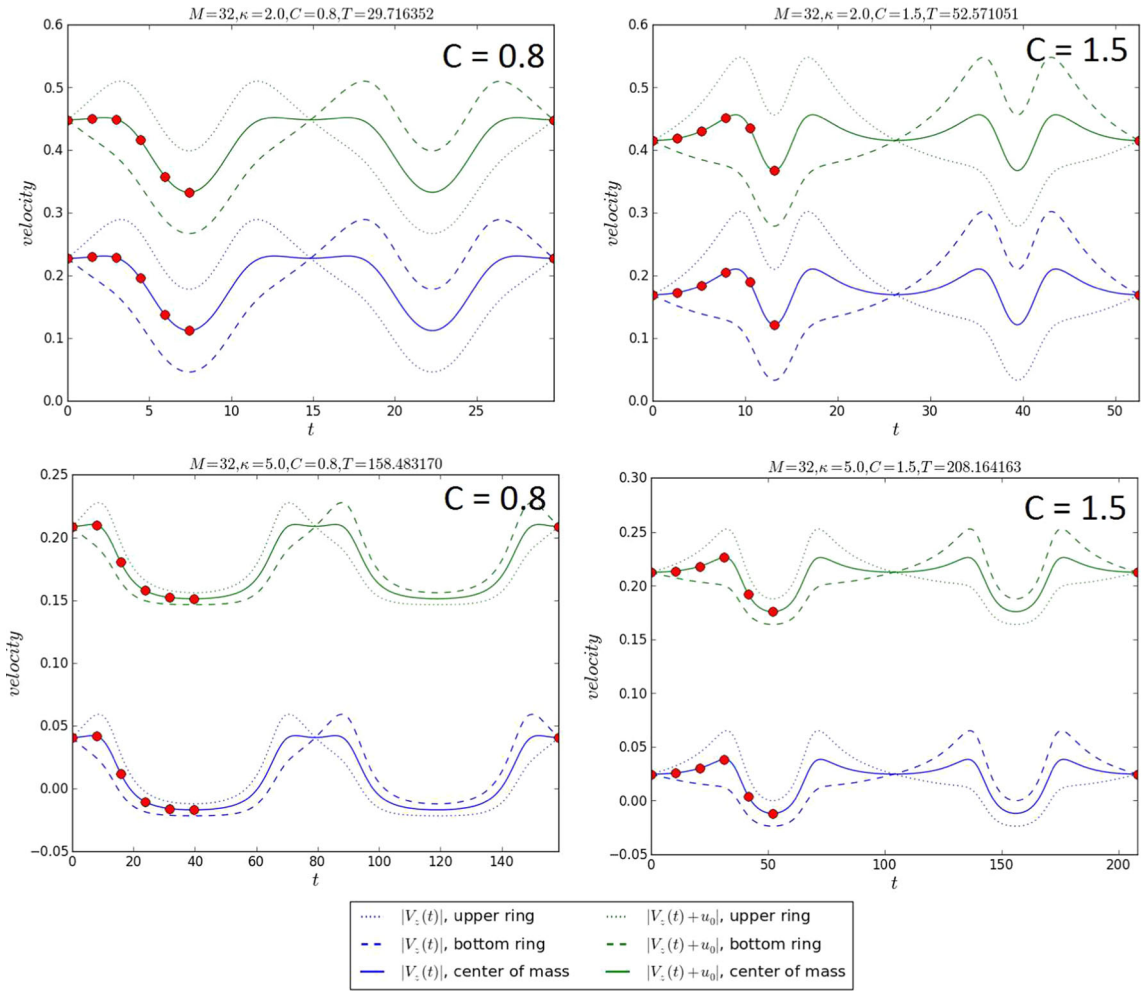

Fig. 16 The settling velocity $|V_z(t)|$ (blue lines) and $|V_z(t) + u_0|$ (green lines) for periodic motions of each ring and the center-of-mass velocity for the system of two rings with $N = 32$. Left: $C = 0.8$, right: $C = 1.5$. The periods T are indicated in the panel titles. The time-points of $T/20$, $2T/20$, $3T/20$, $4T/20$, $5T/20$ are marked with red dots

Settling velocities of two rings and four rings made of the same number of particles and performing periodic motions from the 1st, 2nd, and 3rd family are compared in Fig. 17. Settling is slower for greater κ (compare Fig. 17A to decreasing permeability in Figs. 17B–D). For all values of κ it can be observed that the 2nd periodic solution leads to the fastest settling, 1st to an intermediate, and 3rd to the smallest. This order is not changed in media of different permeability. For greater values of κ (Fig. 17C, D) not all types of periodic solutions were found. The settling velocity of two rings is comparable to the one of 2nd solution of a 4-rings system.

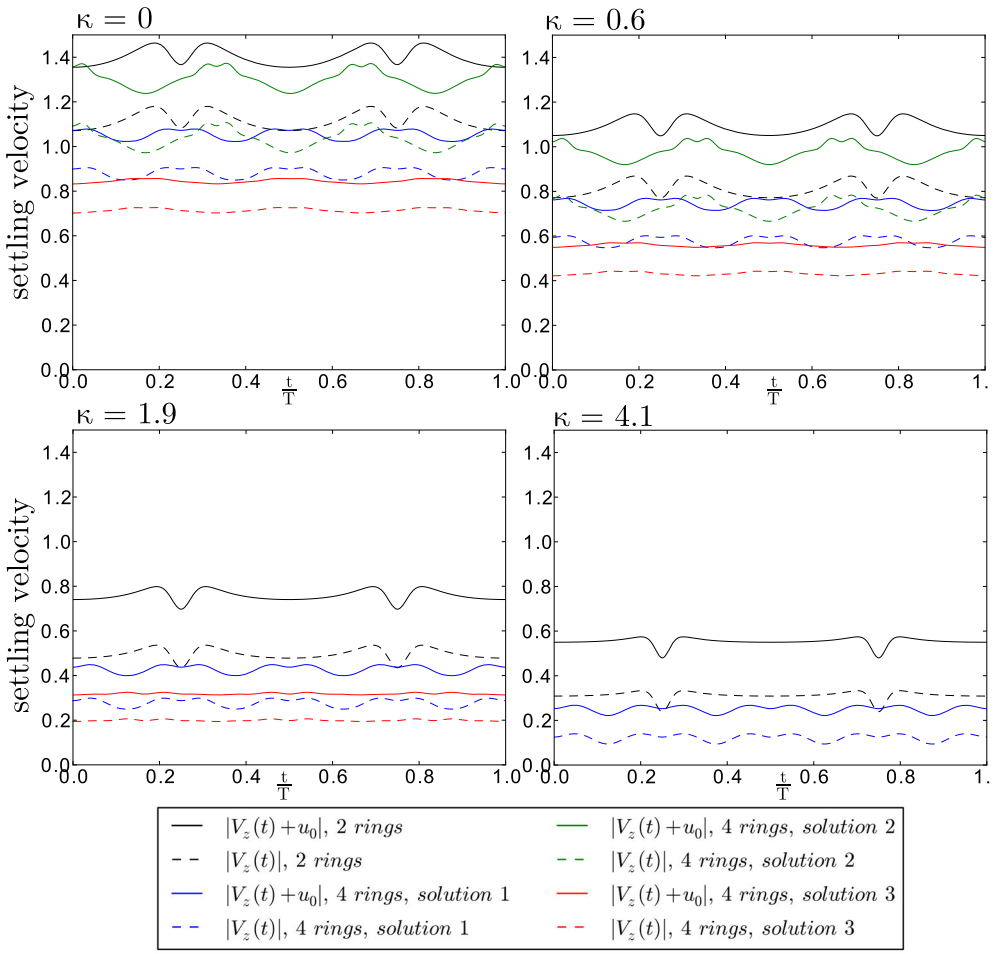

Fig. 17 Comparison of settling velocities of systems made of 2 and 4 rings for different values of κ. Velocity values are shown both without self-term (dashed lines) and with the self-term (solid lines). The colors blue, green, and red correspond to 3 different types of periodic solution for the 4-rings system, while black lines denote values for the system of two rings with the same $N = 256$ and $C = 1.5$

References

1. Molnar, I.L., Pensini, E., Asad, M.A., Mitchell, C.A., Nitsche, L.C., Pyrak-Nolte, L.J., Miño, G.L., Krol, M.M.: Colloid transport in porous media: a review of classical mechanisms and emerging topics. Transp. Porous Med. 1–28 (2019)
2. Boomsma, E., Pyrak-Nolte, L.J.: In Dynamics of Fluids and Transport in Complex Fractured-Porous Systems. In: Faybishenko, B., Benson, S. M., Gale, J.E. (eds.), (American Geophysical Union, 2015), vol. 210 of Geophysical Monograph Book Series, pp. 65–84. ISBN 978-1-118-87728-9; 978-1-118-87720-3
3. Molnar, I.L., Johnson, W.P., Gerhard, J.I., Willson, C.S., O'Carroll, D.M.: Predicting colloid transport through saturated porous media: a critical review. Water Resour. Res. **51**, 6804 (2015)
4. Spagnolie, S.E., Underhill, P.T.: Swimming in complex fluids. Annu. Rev. Condensed Matter Phys. **14**, 381 (2023)
5. Brinkman, H.C.: A calculation of the viscosity and the sedimentation velocity for solutions of large chain molecules taking into account the hampered flow of the solvent through each chain molecule. Proc. R. Dutch Acad. Sci. **50**, 821 (1947)
6. Debye, P., Büche, A.M.: Intrinsic viscosity, diffusion, and sedimentation rate of polymers in solution. J. Chem. Phys. **16**, 573 (1948)
7. Durlofsky, L., Brady, J.: Analysis of the Brinkman equation as a model for flow in porous media. Phys. Fluids **30**, 3329 (1987)
8. Kang, K., Wilk, A., Buitenhuis, J., Patkowski, A., Dhont, J.K.: Diffusion of spheres in isotropic and nematic suspensions of rods. J. Chem. Phys. **124** (2006)
9. Cichocki, B., Ekiel-Jeżewska, M.L.: Self-diffusion of a sphere in an effective medium of rods. J. Chem. Phys. **130** (2009)
10. Bechinger, C., Di Leonardo, R., Löwen, H., Reichhardt, C., Volpe, G., Volpe, G.: Active particles in complex and crowded environments. Rev. Mod. Phys. **88**, 045006 (2016)
11. Nganguia, H., Pak, O.S.: Squirming motion in a Brinkman medium. J. Fluid Mech. **855**, 554 (2018)

12. Nganguia, H., Zhu, L., Palaniappan, D., Pak, O.S.: Squirming in a viscous fluid enclosed by a Brinkman medium. Phys. Rev. E **101**, 063105 (2020)
13. Jánosi, I.M., Tél, T., Wolf, D.E., Gallas, J.A.: Chaotic particle dynamics in viscous flows: the three-particle Stokeslet problem. Phys. Rev. E **56**, 2858 (1997)
14. Ekiel-Jeżewska, M.L.: Class of periodic and quasiperiodic trajectories of particles settling under gravity in a viscous fluid. Phys. Rev. E **90**, 043007 (2014)
15. Gruca, M., Bukowicki, M., Ekiel-Jeżewska, M.L.: Periodic and quasiperiodic motions of many particles falling in a viscous fluid. Phys. Rev. E **92**, 023026 (2015)
16. Gruca, M.: Motion of regular systems of many particles interacting hydrodynamically under gravity, Ph.D. Thesis (Institute of Fundamental Technological Research, Polish Academy of Sciences) (2016)
17. Jayaweera, K., Mason, B., Slack, G.: The behaviour of clusters of spheres falling in a viscous fluid Part 1. Exp. J. Fluid Mech. **20**, 121 (1964)
18. Hocking, L.: The behaviour of clusters of spheres falling in a viscous fluid Part 2. Slow motion theory. J. Fluid Mech. **20**, 129 (1964)
19. Kamel, M., Tory, E.: Sedimentation of clusters of identical spheres II. Periodic motion of three spheres. Powder Technol. **63**, 187 (1990)
20. Koglin,B., Al Taweel,A.: Geometrical Configuration and Settling Velocity of Clusters Settling in Fluids and Suspensions. In Harold Heywood Memorial Symposium, Loughborough (1973)
21. Tory, E., Kamel, M., Tory, C.: Sedimentation of clusters of identical spheres III. Periodic motion of four spheres. Powder Technol. **67**, 71 (1991)
22. Golubitsky, M., Krupa, M., Lim, C.: Time-reversibility and particle sedimentation. SIAM J. Appl. Math. **51**, 49 (1991)
23. Tory, E.M., Kamel, M.T.: A note on the periodic motion of four spheres. Powder Technol. **73**, 95 (1992)
24. Lim, C.C., McComb, I.-H.: Stability of normal modes and subharmonic bifurcations in the 3-body Stokeslet problem. J. Differ. Equ. **121**, 384 (1995)
25. Snook, I., Briggs, K., Smith, E.: Hydrodynamic interactions and some new periodic structures in three particle sediments. Phys. A **240**, 547 (1997)
26. Bargieł, M., Kamel, M.T., Tory, E.M.: Periodic motion of four spheres in a"kite"configuration. Powder Technol. **214**, 14 (2011)
27. Bargieł, M., Tory, E.M.: Effect of higher-order and lubrication terms on the stability of polygonal arrangements of sedimenting spheres. Powder Technol. **264**, 519 (2014)
28. Ekiel-Jeżewska, M., Felderhof, B.: Periodic sedimentation of three particles in periodic boundary conditions. Phys. Fluids **17** (2005)
29. Ekiel-Jeżewska, M., Felderhof, B.: Clusters of particles falling in a viscous fluid with periodic boundary conditions. Phys. Fluids **18** (2006)
30. Caflisch, R.E., Lim, C., Luke, J.H., Sangani, A.S.: Periodic solutions for three sedimenting spheres. Phys. Fluids **31**, 3175 (1988)
31. Ekiel-Jeżewska, M.L., Gubiec, T., Szymczak, P.: Stokesian dynamics of close particles. Phys. Fluids **20** (2008)
32. Chajwa, R., Menon, N., Ramaswamy, S.: Kepler orbits in pairs of disks settling in a viscous fluid. Phys. Rev. Lett. **122**, 224501 (2019)
33. Jung, S., Spagnolie, S., Parikh, K., Shelley, M., Tornberg, A.-K.: Periodic sedimentation in a Stokesian fluid. Phys. Rev. E **74**, 035302 (2006)
34. Ekiel-Jeżewska, M.L., Wajnryb, E.: Lifetime of a cluster of spheres settling under gravity in Stokes flow. Phys. Rev. E **83**, 067301 (2011)
35. Kim, S., Karrila, S.J.: Microhydrodynamics: Principles and Selected Applications. Dover Publications Inc, New York (2005)
36. Tchen, C.-M.: Motion of small particles in skew shape suspended in a viscous liquid. J. Appl. Phys. **25**, 463 (1954)
37. Cox, R.: The motion of long slender bodies in a viscous fluid part 1. General theory. J. Fluid Mech. **44**, 791 (1970)
38. Majumdar, S., O'Neill, M.: On axisymmetric Stokes flow past a torus. Z. Angew. Math. Phys. **28**, 541 (1977)
39. Goren, S.L., O'Neill, M.E.: Asymmetric creeping motion of an open torus. J. Fluid Mech. **101**, 97 (1980)
40. Nitsche, J., Batchelor, G.: Break-up of a falling drop containing dispersed particles. J. Fluid Mech. **340**, 161 (1997)
41. Machu, G., Meile, W., Nitsche, L.C., Schaflinger, U.: Coalescence, torus formation and breakup of sedimenting drops: experiments and computer simulations. J. Fluid Mech. **447**, 299 (2001)
42. Metzger, B., Nicolas, M., Guazzelli, E.: Falling clouds of particles in viscous fluids. J. Fluid Mech. **580**, 283 (2007)
43. Myłyk, A., Ekiel-Jeżewska, M.L.: How walls influence destabilization of a suspension drop settling under gravity in a viscous fluid? Colloid Surface A **365**, 109 (2010)
44. Myłyk, A., Meile, W., Brenn, G., Ekiel-Jeżewska, M.L.: Break-up of suspension drops settling under gravity in a viscous fluid close to a vertical wall. Phys. Fluids **23**, 063302 (2011)